Supporting Information for

Hydrologic regulation of clay-mineral transformations in a redoximorphic soil of subtropical monsoonal China

Lulu Zhao [a], Hanlie Hong [a, *], Qian Fang [a, *], Hetang Hei [b], Thomas J. Algeo [a, c, d]

[a] *State Key Laboratory of Biogeology and Environmental Geology, Hubei Key Laboratory of Critical Zone Evolution, School of Earth Sciences, China University of Geosciences, Wuhan 430074, China*

[b] *Yunnan Earthquake Agency, Kunming 650224, China*

[c] *Department of Geology, University of Cincinnati, Cincinnati, OH 45221-0013, USA*

[d] *State Key Laboratory of Geological Processes and Mineral Resources, China University of Geosciences, Wuhan 430074, China*

Contents of this file

Table S1. Pedogenic forms of Fe and Al in SZ section

Horizon	Depth	Al_p	Fe_p	Al_o	Fe_o	Al_d	Fe_d	Alt	Fet	Al_o/Fe_o	Fe_o/Fe_d	Al_d-Al_o	Fe_d-Fe_o
	m	g kg^{-1}										g kg^{-1}	
HH	0.3	0.49	0.22	1.03	2.38	1.25	9.22	74.72	38.58	0.82	0.26	0.23	6.83
	0.9	0.37	0.14	1.03	2.82	1.53	11.53	75.39	39.70	0.67	0.24	0.51	8.70
	1.2	0.32	0.16	0.92	2.34	1.55	13.37	75.80	41.52	0.59	0.18	0.64	11.03
	1.5	0.28	0.13	0.98	2.46	1.46	13.58	84.52	46.77	0.67	0.18	0.48	11.12
	1.8	0.35	0.17	0.79	1.97	1.48	13.40	82.16	45.27	0.53	0.15	0.69	11.43
RH	2.1	0.33	0.20	0.85	2.63	1.51	13.31	83.65	45.59	0.56	0.20	0.67	10.68
	2.4	0.42	0.26	0.89	2.27	1.53	14.22	78.68	45.21	0.58	0.16	0.65	11.96
	3.0	0.30	0.15	1.00	2.72	1.51	15.47	79.93	45.30	0.66	0.18	0.52	12.76
	3.3	0.28	0.15	0.88	2.45	1.48	16.20	80.61	44.69	0.60	0.15	0.59	13.75
	3.6	0.35	0.23	0.70	1.69	1.52	14.26	77.28	42.49	0.46	0.12	0.81	12.58
	3.9	0.43	0.26	0.80	2.12	1.59	14.38	74.02	40.61	0.51	0.15	0.78	12.26
	4.2	0.21	0.14	0.67	1.63	1.70	15.50	77.63	41.85	0.40	0.11	1.03	13.87
	4.5	0.27	0.15	0.79	1.55	1.68	14.39	74.65	39.63	0.47	0.11	0.89	12.85
	5.1	0.23	0.14	0.74	1.61	1.75	14.76	70.93	39.05	0.42	0.11	1.01	13.15
	5.4	0.29	0.14	0.64	1.27	1.57	13.63	69.77	38.53	0.41	0.09	0.93	12.36
BL	6.0	0.22	0.13	0.53	1.12	1.66	13.88	65.97	35.92	0.32	0.08	1.13	12.76
	6.9	0.18	0.13	0.48	1.01	1.61	14.06	62.49	38.17	0.29	0.07	1.14	13.06

Table S2. Trace elements and REE geochemistry data (in ppm) for representative bulk samples in HH, PH, and BL

Horizon	HH					RH							BL	
Depth (m)	0.3	0.9	1.2	1.5	1.8	2.1	2.4	3.3	3.6	3.9	4.2	5.1	6.0	7.2
Li	46.2	48.1	47.0	41.6	46.0	50.3	47.3	48.7	52.0	48.8	49.5	44.5	41.7	41.4
Be	2.06	2.17	2.07	2.46	2.45	2.53	2.33	2.11	2.08	2.01	1.96	1.92	1.64	1.40
Sc	13.2	13.1	13.3	14.2	14.3	14.4	13.8	13.9	13.5	12.6	13.2	12.8	11.6	10.4
V	105	107	109	116	115	116	113	117	114	108	111	104	98.0	93.1
Cr	82.0	83.5	81.0	85.4	84.4	89.9	86.2	88.3	101	83.9	85.2	85.3	91.3	104
Co	14.6	17.4	20.5	20.5	19.7	22.2	14.5	18.9	27.8	29.4	18.6	16.4	12.6	8.09
Ni	39.0	37.1	40.8	37.4	37.6	41.3	37.5	37.6	36.4	36.1	38.5	33.7	31.6	24.9
Cu	27.1	28.5	27.8	28.9	29.3	31.2	29.8	28.5	29.8	28.6	28.8	27.0	23.2	21.4
Zn	71.0	75.7	75.4	73.5	75.2	78.7	73.8	65.1	68.9	66.6	68.3	67.2	63.0	58.4
Ga	18.2	18.7	19.0	20.7	20.4	20.6	19.6	20.2	19.7	18.5	19.3	17.8	16.4	14.9
Rb	114	120	121	128	129	129	124	118	121	115	116	112	102	91.7
Sr	60.7	57.9	55.9	55.7	57.1	57.3	56.3	51.9	51.3	50.9	50.7	50.6	48.0	46.7
Y	30.5	27.5	25.5	25.1	28.6	29.4	28.0	28.1	29.4	29.2	26.7	27.6	27.8	29.8
Zr	298	291	292	276	280	275	289	294	307	311	293	312	332	373
Nb	20.8	21.0	21.0	20.3	20.2	20.5	20.6	21.2	21.7	21.4	21.2	21.2	21.9	22.3
Sn	3.05	3.15	3.11	3.30	3.35	3.37	3.26	3.33	3.34	3.36	3.33	3.13	3.15	2.92
Cs	8.69	9.49	9.68	10.4	10.1	10.3	9.80	9.76	9.84	9.52	9.97	9.26	8.71	8.85
Ba	479	489	471	494	488	494	469	441	434	408	400	388	337	270
La	37.6	36.5	35.3	33.8	36.0	37.6	38.6	36.6	36.9	36.7	35.7	36.9	33.3	36.3
Ce	97.9	86.1	87.3	80.6	74.3	86.5	83.8	82.6	83.6	84.0	76.2	73.9	66.3	62.2
Pr	8.09	7.76	7.43	6.97	7.57	8.13	8.07	7.67	7.63	7.57	7.42	7.67	6.86	7.44
Nd	31.5	28.9	26.9	25.4	27.2	30.0	29.7	28.4	28.3	27.9	27.5	28.2	24.8	26.4
Sm	5.73	5.18	4.85	4.64	5.11	5.61	5.58	5.02	5.00	5.02	4.69	5.17	4.58	4.65
Eu	1.11	0.93	0.85	0.90	0.97	1.09	1.05	0.93	0.93	0.94	0.87	0.95	0.79	0.84
Gd	4.92	4.41	3.88	3.94	4.31	4.64	4.47	4.03	4.23	4.01	3.98	4.21	3.86	4.08
Tb	0.82	0.75	0.68	0.67	0.73	0.77	0.77	0.73	0.73	0.71	0.69	0.73	0.68	0.72
Dy	4.91	4.41	4.25	4.18	4.73	4.84	4.64	4.37	4.71	4.53	4.37	4.61	4.41	4.57
Ho	1.01	0.95	0.91	0.89	0.97	1.00	0.95	0.93	0.98	0.96	0.93	0.94	0.93	0.95
Er	2.95	2.88	2.64	2.68	2.83	2.86	2.83	2.80	2.90	2.95	2.72	2.80	2.71	2.87
Tm	0.45	0.45	0.42	0.42	0.43	0.47	0.46	0.45	0.47	0.46	0.44	0.45	0.45	0.47
Yb	2.96	3.05	2.84	2.77	3.05	2.94	3.03	2.96	3.17	3.16	2.89	3.00	3.04	3.16
Lu	0.44	0.43	0.40	0.40	0.43	0.42	0.41	0.43	0.44	0.45	0.43	0.44	0.42	0.47
Hf	8.06	8.01	7.99	7.65	7.78	7.59	7.83	8.20	8.25	8.42	7.95	8.61	8.88	9.71
Ta	1.55	1.56	1.52	1.47	1.55	1.50	1.50	1.52	1.53	1.58	1.56	1.53	1.58	1.60
Tl	0.97	1.08	0.99	1.13	1.06	1.12	1.02	1.02	1.06	0.98	1.01	0.98	0.91	0.92
Pb	23.6	26.4	29.3	29.8	26.7	28.2	26.2	27.2	29.6	32.6	23.9	25.5	18.7	15.6
Th	16.1	16.2	16.8	17.3	17.0	16.8	16.4	17.0	16.6	16.3	16.9	15.8	15.2	15.1
U	3.93	4.12	4.15	4.18	4.13	4.30	4.34	4.50	4.51	4.21	4.23	4.29	4.14	4.15

Table S3. Fitting parameters of the deconvoluted peaks in the XRD patterns

Depth (m)	Assignment	Position [°2θ]	d-spacing [Å]	Height [cts]	Left FWHM [°2θ]	Relative intensity [%]
0.3	HIV	6.23	14.19	250	0.40	24
	I-S / I-V	6.67	12.56	73	0.84	7
	Illite	8.80	10.06	366	0.62	35
	Kaolinite	12.35	7.12	362	0.46	34
1.1	HIV	6.33	14.17	87	0.34	15
	I-S / I-V	6.70	12.70	31	0.97	5
	Illite	8.90	10.09	220	0.65	38
	K-S	11.36	7.85	27	0.22	5
	Kaolinite	12.51	7.18	213	0.62	37
1.8	HIV	6.17	14.32	35	0.45	6
	Illite	8.76	10.09	292	0.98	50
	K-S	11.55	7.54	48	0.93	8
	Kaolinite	12.20	7.25	205	0.52	35
3.3	Illite	8.79	10.05	191	0.71	42
	K-S	11.38	7.80	79	0.78	22
	Kaolinite	12.34	7.17	174	0.63	36
5.1	I-S / I-V	6.64	13.10	13	0.81	3
	Illite	8.85	10.07	117	0.79	27
	K-S	11.63	7.67	115	1.27	27
	Kaolinite	12.45	7.17	193	0.84	45
7.1	Smectite	5.58	16.96	52	0.70	11
	I-S / I-V	6.58	13.20	45	0.76	9
	Illite	8.88	10.03	90	0.91	18
	K-S	11.82	7.55	125	1.27	25
	Kaolinite	12.47	7.16	181	0.86	37

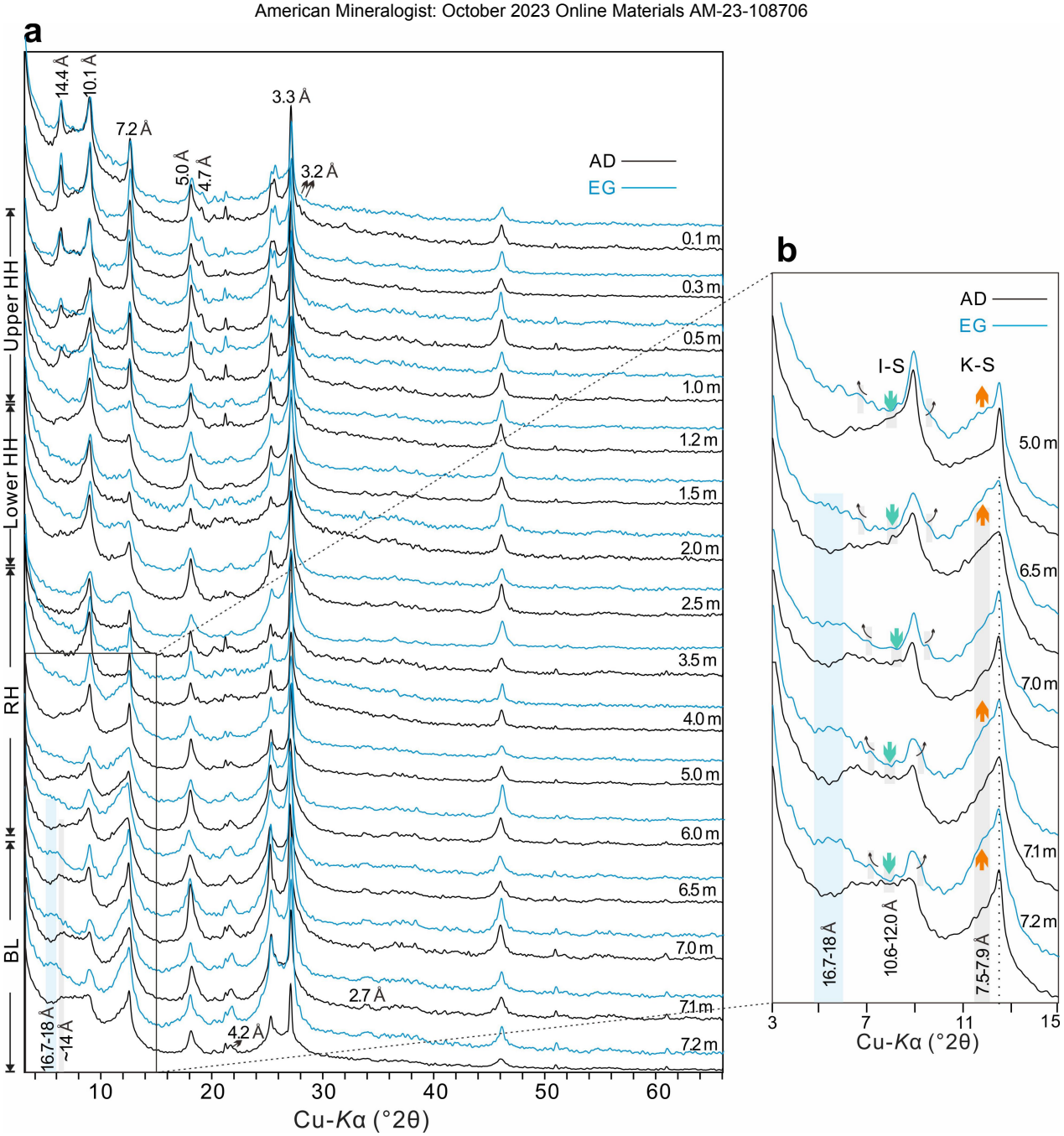

Figure S1. Representative XRD patterns of clay fractions (AD and EG treatment) from the HH, RH, and BL. AD = Air dried treatment; EG = ethylene glycol solvation. Green arrows indicate the position of I-S (001) reflection in AD, and orange arrows indicate the position of K-S (001) reflection in AD. Black arrows indicate general moving direction of I-S (001) reflection after EG treatment.

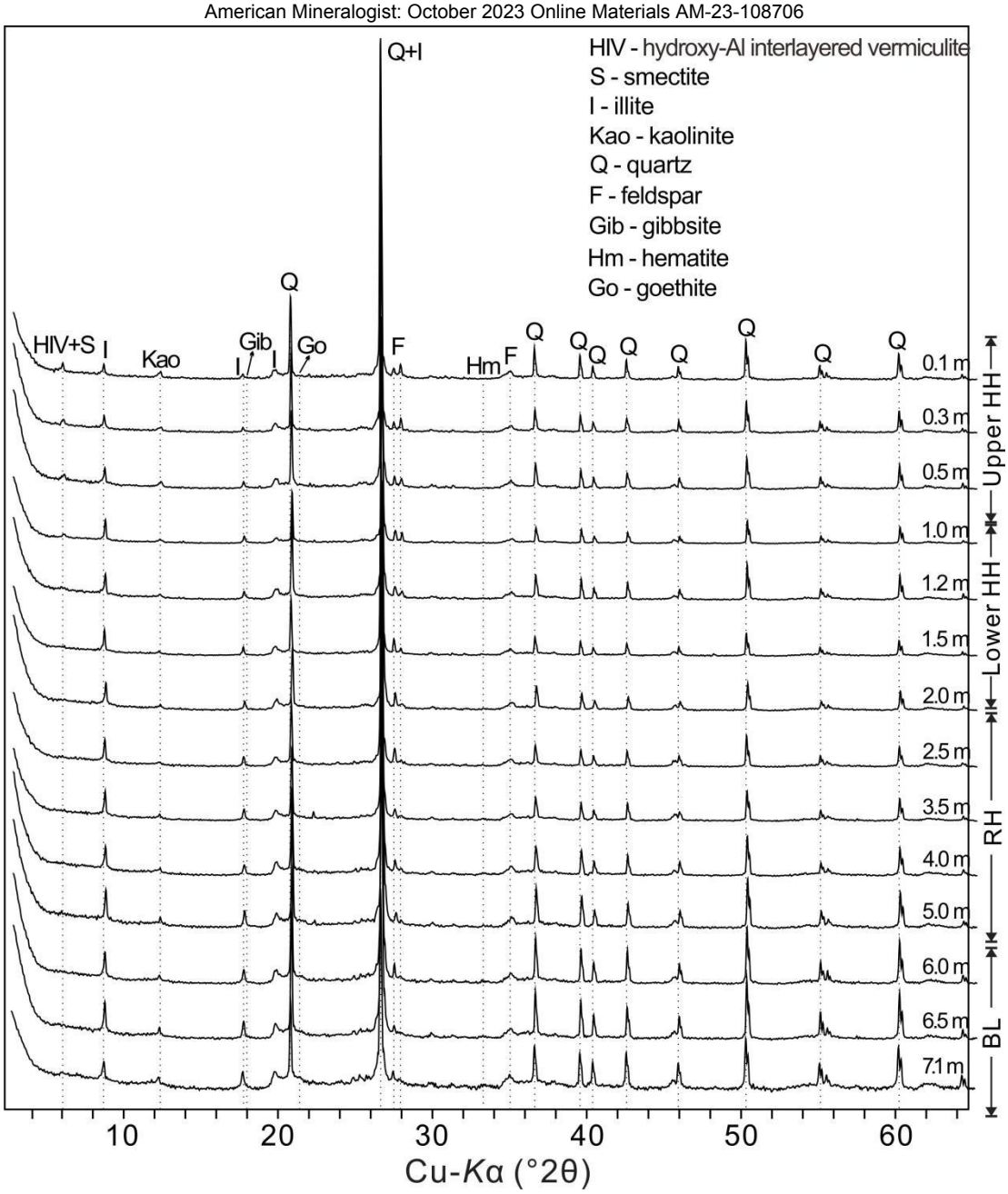

Figure S2. XRD pattern of the randomly-oriented powder mounts for representative soil samples (<74 μm) in homogenous horizon (HH), redoximorphic horizon (RH), and basal layer (BL).

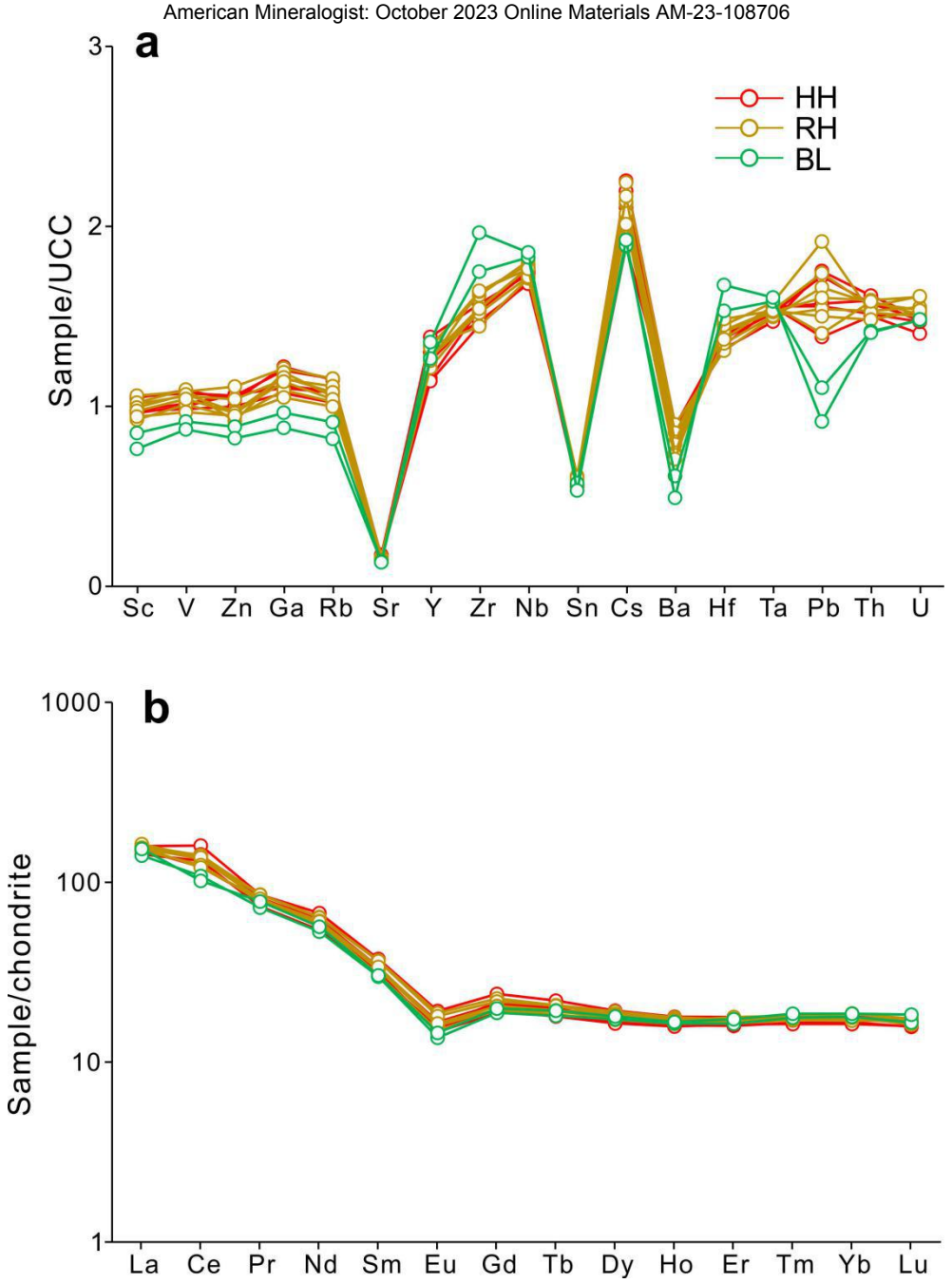

Figure S3. a) UCC-normalized distributions of trace elements, and b) chondrite-normalized REEs in the SZ section. The chondrite-normalized REEs show highly similar distribution patterns, which may provide as evidence for quasi-uniform compositions of eolian parent materials.

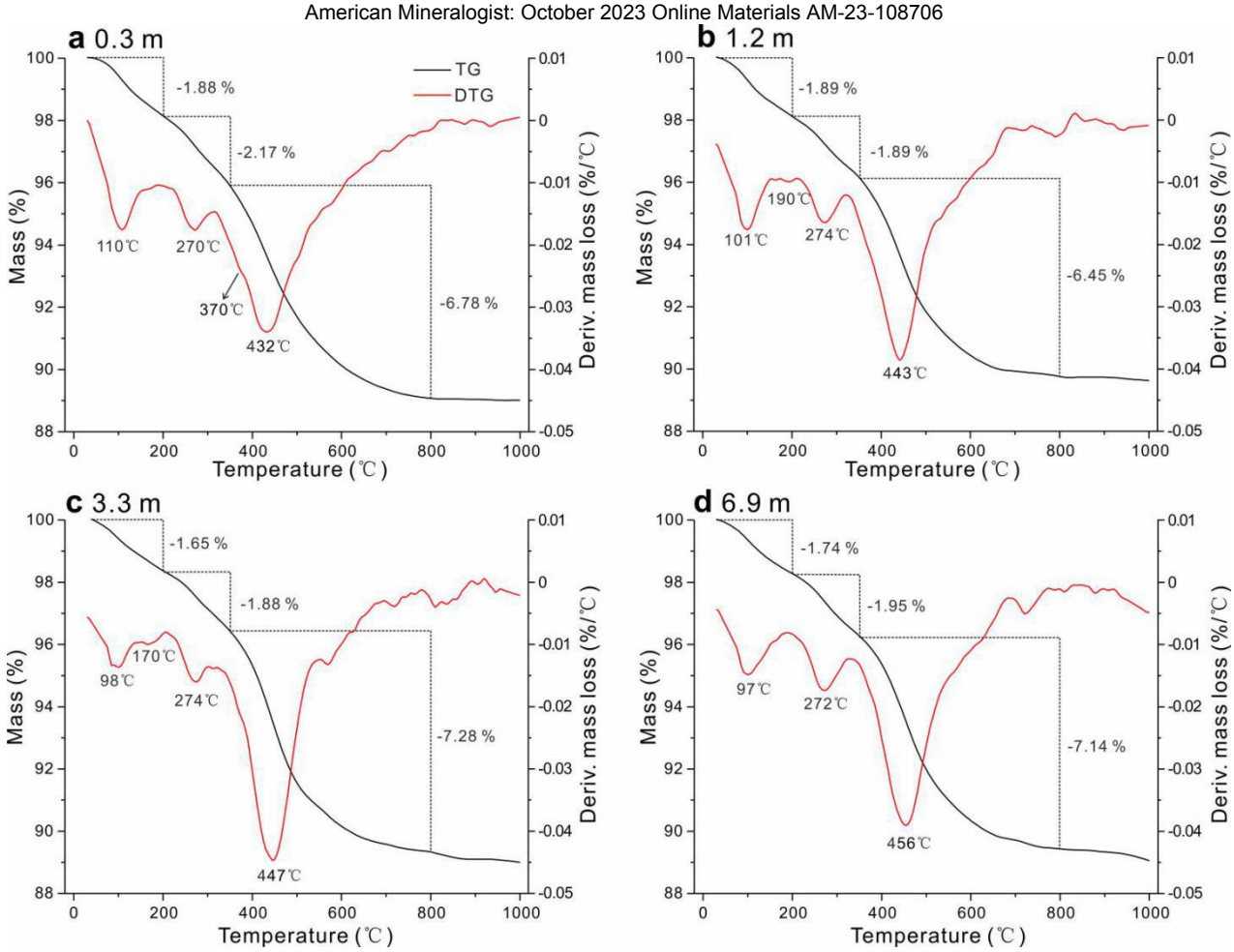

Figure S4. Thermogravimetric analysis (TG-DTG) curves of the clay-fraction samples from (a-b) HH (0.3 m and 1.2 m), (c) RH (3.3 m), (d) BL (6.9 m). A minor endothermic peak at 370 °C can only be found in the DTA patterns of the HH samples, providing as another line of evidence for the presence of HIV in the HH.

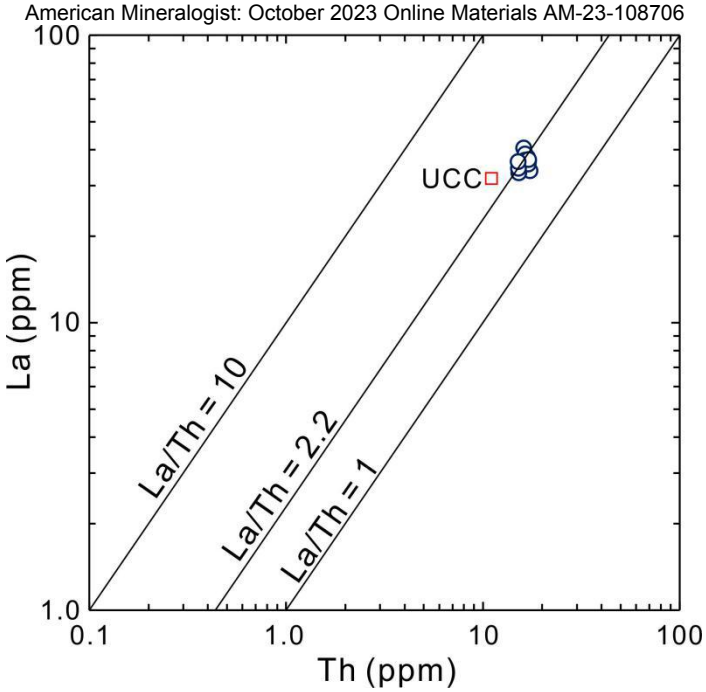

Figure S5. La-Th covariation for SZ section. UCC (red square; McLennan, 2001) is plotted for comparison. The nearly constant La-Th concentrations indicate that the SZ soils are derived from a nearly homogenous source.